Conformational Characteristics and Configurational Properties of Poly(ethylene oxide-*alt*-ethylene sulfide)

Yuji Sasanuma,* Shunsuke Asai, and Ryota Kumagai

Department of Applied Chemistry and Biotechnology, Faculty of Engineering, Chiba University, 1-33 Yayoi-cho, Inage-ku, Chiba 263-8522, Japan

Received January 9, 2007; Revised Manuscript Received February 7, 2007

ABSTRACT: Conformational analysis of poly(ethylene oxide-*alt*-ethylene sulfide) (PEOES) has been carried out by ab initio molecular orbital (MO) calculations for a model compound, 2-methoxyethyl methyl sulfide (MEMS), and a refined rotational isomeric state (RIS) scheme developed here. The refined RIS scheme, including the dependence of geometrical parameters as well as interaction energies on conformations of the current and neighboring bonds, is formulated herein. Experimental observations of bond conformations of MEMS and the dipole moment ratio and its temperature coefficient of PEOES in benzene were exactly reproduced by the completely theoretical treatment of the MO−RIS calculations. Thermodynamic and solution properties and weak interactions of PEOES are discussed and compared with those of poly(ethylene oxide) and poly(ethylene sulfide).

1. Introduction

Physical chemists may have an ideal to elucidate all chemical phenomena quantitatively on the basis of the first principles, that is, the Schrödinger equation. In polymer science, however, this ideal has been regarded as chasing after rainbows, because polymers are too large to be directly dealt with by quantum mechanics. Even a single polymeric chain has an astronomical number of degrees of freedom in conformation and configuration. Statistical mechanics fulfills a role of the bridge between microscopic and macroscopic phenomena; rigorous solutions of quantum theory for a small molecule may be extended to canonical ensemble averages of thermodynamics.

Simple models for polymeric chains have been proposed: for example, the freely jointed chain, the freely rotating chain, and the chain with hindered rotation.[1] In this order, the chain flexibility is reduced, and the models become realistic. The extension of this line may reach the rotational isomeric state (RIS) model,[1,2] in which the internal rotations are interdependent and expressed as a function of the Boltzmann factors of conformational energies under the RIS approximation. The RIS scheme has been applied to a number of synthetic and biological polymers to evaluate a variety of configurational properties.[1,2] However, the RIS scheme still leaves room for improvement. The geometrical parameters depend on conformations of not only the current but also neighboring bonds; nevertheless, the RIS model (referred here to as the *conventional* RIS model) does not include the latter dependence. The bond length, bond angle, and dihedral angle of, for example, poly(ethylene oxide-*alt*-ethylene sulfide) (PEOES, see Figure 1a) treated here, depending on conformations of the adjacent bonds, may vary within allowances of, at most, 0.016 Å, 7.7°, and 42.2°, respectively (Table 1). The bond length is rigid, whereas the dihedral angle is very flexible. In this paper, an improved RIS scheme is proposed and formulated so that the geometrical parameters can be changed as a function of conformations of the current and adjacent bonds (it is hereafter referred to as the *refined* RIS scheme).

* Corresponding author. E-mail: sasanuma@facutly.chiba-u.jp. Fax: +81 43 290 3394.

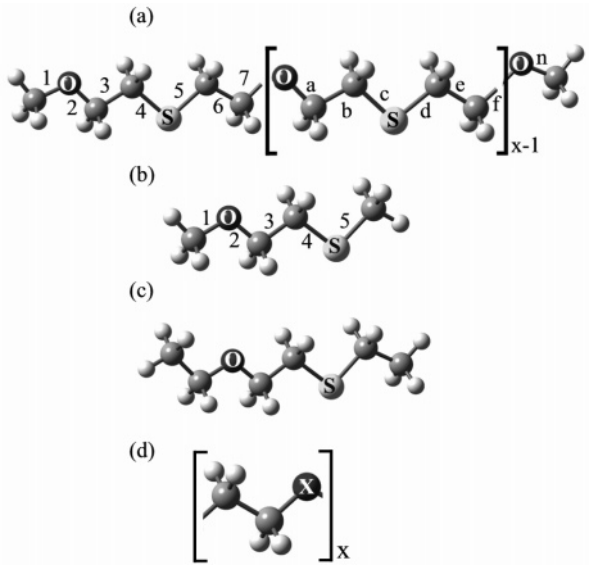

Figure 1. All-trans conformations of (a) poly(ethylene oxide-*alt*-ethylene sulfide) (PEOES), (b) 2-methoxyethyl methyl sulfide (MEMS), (c) 2-ethoxyethyl ethyl sulfide (EEES), and (d) poly(ethylene oxide) (PEO, X = O) or poly(ethylene sulfide) (PES, X = S). The bonds are labeled as indicated.

This study has dealt with conformational analysis of PEOES as an application of the refined RIS scheme. Poly(ethylene oxide) (PEO) and poly(ethylene sulfide) (PES) exhibit characteristic weak interactions: PEO, the (C−H)···O attraction;[3−5] PES, the dipole−dipole attraction.[3,5,6] It is of interest to investigate whether these interactions can also be found in PEOES and how they affect its structures and properties. Ab initio molecular orbital (MO) calculations with and without solvent effects were carried out for a model compound of PEOES, 2-methoxyethyl methyl sulfide (MEMS, see Figure 1b), its intramolecular interactions were investigated, and the conformational energies were evaluated. With the conformational energies thus obtained and the geometrical parameters optimized by the density functional calculations for 2-ethoxyethyl ethyl sulfide (EEES, see Figure 1c), the refined RIS model was

10.1021/ma070065n CCC: $37.00
Published on Web 03/29/2007

Table 1. Geometrical Parameters of PEOES, Used in the Refined RIS Calculations[a]

conformation [b]						
α	β	γ	l_j [c]	θ_{j-1} [d]	θ_j [e]	ϕ_j [f]
			Bond a			
t	t	t	1.416	112.9	107.4	0.0
t	g^+	t	1.419	114.7	112.3	99.0
g^+	t	t	1.419	114.4	107.1	7.6
g^+	g^+	t	1.421	114.9	110.9	90.4
g^+	g^-	t	1.423	115.8	110.3	−68.1
t	t	g^+	1.414	113.0	109.1	−3.0
t	g^+	g^+	1.415	114.7	114.8	110.1
t	g^-	g^+	1.416	115.7	114.4	−84.4
g^+	t	g^+	1.416	114.5	108.8	2.9
g^+	g^+	g^+	1.418	115.4	113.8	100.0
g^+	g^-	g^+				
g^-	t	g^+	1.416	114.6	108.7	−9.8
g^-	g^+	g^+	1.419	116.5	113.9	79.1
g^-	g^-	g^+				
			Bond b			
t	t	t	1.525		110.1	0.0
t	g^+	t	1.521		111.2	118.2
g^+	t	t	1.533		109.8	3.1
g^+	g^+	t	1.531		110.9	126.4
g^+	g^-	t	1.533		113.7	−105.4
t	t	g^+	1.525		113.7	0.3
t	g^+	g^+	1.524		115.5	110.9
t	g^-	g^+	1.523		115.8	−109.7
g^+	t	g^+	1.534		113.5	4.2
g^+	g^+	g^+	1.537		116.3	132.5
g^+	g^-	g^+				
g^-	t	g^+	1.534		113.6	−2.5
g^-	g^+	g^+				
g^-	g^-	g^+	1.532		115.8	−110.1
			Bond c			
t	t	t	1.836		99.4	0.0
t	g^+	t	1.833		101.3	101.7
g^+	t	t	1.841		99.4	19.5
g^+	g^+	t	1.837		100.4	99.4
g^+	g^-	t	1.837		102.0	−100.3
t	t	g^+	1.838		100.7	10.0
t	g^+	g^+	1.835		101.8	98.1
t	g^-	g^+	1.839		102.4	−79.7
g^+	t	g^+	1.842		100.5	23.2
g^+	g^+	g^+	1.839		101.4	97.8
g^+	g^-	g^+	1.838		103.6	−104.2
g^-	t	g^+	1.842		100.4	−19.0
g^-	g^+	g^+	1.839		102.9	100.8
g^-	g^-	g^+	1.845		101.5	−71.1

[a] Obtained from the geometrical optimization for EEES at the B3LYP/6-31G(d) level. For each bond, 27 conformers are defined. The geometrical parameters of other conformers are derived from $l_{\alpha\beta\gamma} = l_{\bar{\alpha}\beta\bar{\gamma}}$, $\theta_{\alpha\beta\gamma} = \theta_{\bar{\alpha}\beta\bar{\gamma}}$, and $\phi_{\alpha\beta\gamma} = -\phi_{\bar{\alpha}\beta\bar{\gamma}}$, where the overbar denotes minus sign: $\bar{t} = t$ and $\overline{g^{\pm}} = g^{\mp}$. For bonds d, e, and f, the parameters are obtained from those for bonds c, b, and a, respectively. The blank indicates that the potential minimum was not found there. [b] α, β, and γ represent conformations of bonds $j-1$, j, and $j+1$, respectively. Here, j denotes the current bond. [c] Length of bond j. [d] Angle formed between bonds $j-1$ and j. [e] Angle formed between bonds j and $j+1$. [f] Dihedral angle of bond j. See Figure 4.

applied to PEOES to yield the characteristic ratio, dipole moment ratio, and their temperature coefficients. The above procedure, being a combination of the first-principles (ab initio MO) and statistical mechanics (the refined RIS) computations, does not include any experimental factors. The quantum chemical data on MEMS were transformed by the refined RIS scheme to canonical ensemble averages on PEOES in the gas phase and in the benzene solution. The bond conformations of MEMS and the dipole moment ratio and its temperature coefficient of PEOES were compared with the experimental observations to examine the reliability of the theoretical treatment adopted here. In this paper, thermodynamic and solution properties of PEOES and the weak interactions of

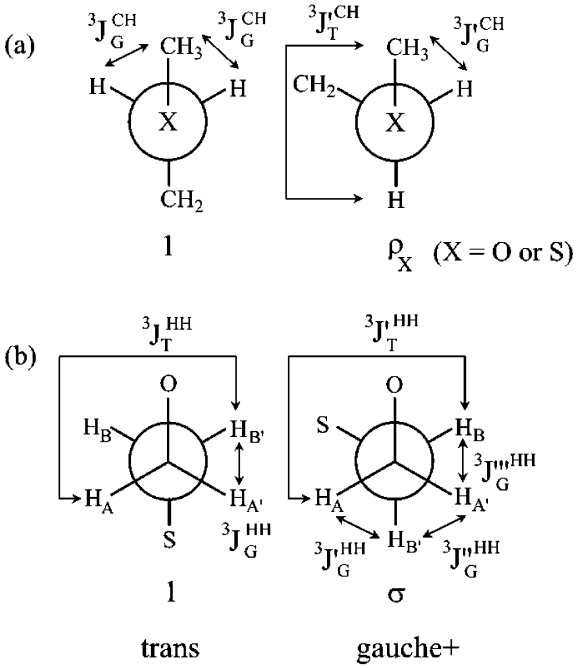

Figure 2. Rotational isomeric states around the (a) X−CH_2 (X = O or S) and (b) CH_2−CH_2 bonds with definitions of vicinal coupling constants. The Greek letters represent first-order interactions.

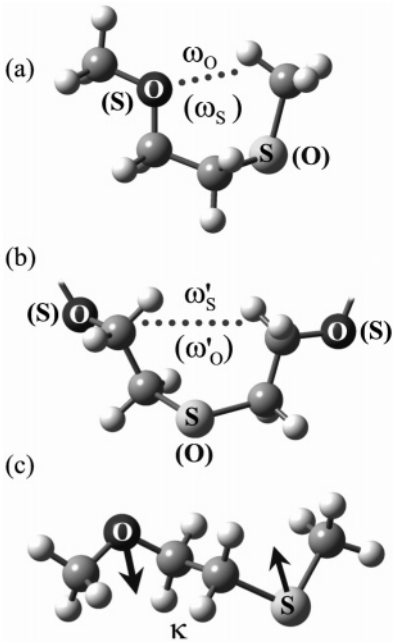

Figure 3. Second- ((a) ω_X and (b) ω'_X, X = O or S) and third-order ((c) κ) intramolecular interactions defined for MEMS and PEOES. The arrows in part c represent dipole moments.

MEMS and PEOES are discussed and compared with those of PEO and PES.

2. Computations and Experiments

2.1. Ab Initio MO Calculations. Ab initio MO calculations were carried out with the Gaussian03 program[7] installed on an HPC Silent-SCC T2 computer. For each conformer of MEMS, the geometrical parameters were fully optimized at the HF/6-31G(d) level, and the thermal correction to the Gibbs free energy (at 25 °C and 1 atm) was calculated with a calibration factor of 0.9135[8] With the optimized geometry, the self-consistent field (SCF) energy was computed at the MP2/6-311+G(3df, 2p) level. All the SCF calculations were performed under the tight convergence. The Gibbs

Table 2. Conformer Free Energies of MEMS, Evaluated from Ab Initio MO Calculations

				ΔG_k[a], kcal mol^{-1}		dipole moment, D	
k	conformation	multiplicity	statistical weight[a]	gas	benzene	μ^{MO} [b]	μ^{BOND} [c]
1	t t t	1	1	0.00	0.00	0.46	0.42
2	t t g$^+$	2	ρ_S	−0.58	−0.58	1.94	1.85
3	t g$^+$ t	2	σ	0.46	0.30	2.13	2.20
4	t g$^+$ g$^+$	2	$\sigma\rho_S$	0.41	0.27	2.78	2.79
5	t g$^+$ g$^-$	2	$\sigma\rho_S\omega_O$	−0.56	−0.35	2.08	1.80
6	g$^+$ t t	2	ρ_O	1.05	0.94	1.85	1.81
7	g$^+$ t g$^+$	2	$\rho_O\rho_S$	0.60	0.52	2.28	2.27
8	g$^+$ t g$^-$	2	$\rho_O\rho_S\kappa$	0.41	0.31	0.34	0.41
9	g$^+$ g$^+$ t	2	$\rho_O\sigma$	1.30	1.12	2.63	2.79
10	g$^+$ g$^+$ g$^+$	2	$\rho_O\sigma\rho_S\chi$	1.25	1.02	1.60	1.78
11	g$^+$ g$^+$ g$^-$	2	$\rho_O\sigma\rho_S\omega_O$	1.10	1.08	2.23	2.15
12	g$^+$ g$^-$ t	2	0				
13	g$^+$ g$^-$ g$^+$	2	0				
14	g$^+$ g$^-$ g$^-$	2	0				

[a] At the MP2/6-311+G(3df, 2p)//HF/6-31G(d) level. Relative to the G_k value of the all-trans conformation. A blank entry indicates that the geometrical optimization did not detect the potential minimum; thus, the conformer is considered to be absent, and the null statistical weight is assigned thereto. For interactions corresponding to the statistical weights, see Figures 2 and 3. [b] At the B3LYP/6-311+G(3df, 2p)//B3LYP/6-31G(d) level. [c] Calculated from $m_{C-O} = 1.13$, $m_{C-C} = 0.00$, and $m_{C-S} = 1.24$ D.

free energy was evaluated from the SCF and thermal-correction energies, being given here as the difference from that of the all-trans conformer and denoted as ΔG_k (k: conformer). Dipole moments and NMR coupling constants of MEMS were evaluated at the B3LYP/6-311+G(3df, 2p)//B3LYP/6-31G(d) and B3LYP/6-311++G(3df, 3pd)//B3LYP/6-31G(d) levels, respectively. The ΔG_k values of MEMS dissolved in benzene were also calculated with the integral equation formalism of the polarizable continuum model (IEF−PCM)[9,10] at the MP2/6-311+G(3df, 2p)//HF/6-31G(d) level. Geometrical parameters of EEES in benzene were optimized at the B3LYP/6-31G(d) level and used in the refined RIS calculations for PEOES.

2.2. Sample Preparation. 2-Methoxyethyl methyl sulfide was prepared from sodium methyl mercaptide and 2-chloroethyl methyl ether.[11] 3-Methyl-1,4-oxathiane (MOT) was prepared as follows.[12] 1,4-Oxathiane reacted with *N*-chlorosuccinimide to afford 3-chloro-1,4-oxathiane. The Grignard reaction between this product and methyl magnesium bromide yielded MOT.

2.3. NMR Measurements. ^{1}H (^{13}C) NMR spectra were measured at 500 MHz (126 MHz) on a JEOL JNM-LA500 spectrometer equipped with a variable temperature controller in the Chemical Analysis Center of Chiba University. During the measurement the probe temperature was maintained within ± 0.1 °C fluctuations. The $\pi/2$ pulse width, data acquisition time, and recycle delay were 5.6 (5.0) μs, 3.3 (2.0) s, and 3.7 (2.0) s, respectively. Here, the values in the parentheses represent the ^{13}C NMR parameters. In the ^{13}C NMR measurements, the gated decoupling technique was employed. Before the Fourier transform, zero filling was conducted so that the digital resolution would be smaller than 0.01 Hz. The solvents were cyclohexane-d_{12} (C_6D_{12}), benzene-d_6 (C_6D_6), chloroform-d ($CDCl_3$), dimethyl-d_6 sulfoxide ($(CD_3)_2SO$), and methanol-d_4 (CD_3OD), and the solute concentration was ca. 5 vol %. The NMR spectra thus obtained were simulated with the gNMR program[13] to derive the chemical shifts and coupling constants.

3. Results

3.1. Conformational Energies of MEMS. Statistical weight matrices, U_j (j: bond number), of MEMS were formulated with reference to those of PEO and PES (see Appendix). The intramolecular interactions are illustrated in Figures 2 and 3. The conformer free energies of MEMS in the gas phase and in the benzene solution, obtained from the MO calculations, are listed in Table 2. The statistical weights are calculated from the conformational energies according to, for example, $\sigma = \exp(-E_\sigma/RT)$, where R is the gas constant, and T is the absolute temperature. The conformational energies of MEMS and PEOES, determined by the least-squares method for the ΔG_k values as described in previous studies,[14] are shown and compared with those of PEO (1,2-dimethoxyethane, DME and triglyme)[4] and PES (1,2-bis(methylthio)ethane, BMTE)[3] in Table 3. Inasmuch as accurate MO calculations on the oxyethylenes have shown a small chain-length dependence of the σ interaction,[4] the conformational energies of DME and triglyme are compared. The conformational energies of PEOES are nearly equal to averages of those of PEO and PES, except for E_{ω_O} and E_{ω_S}. The long C−S bond weakens the (C−H)···O attraction ($|E_{\omega_O}(\text{PEOES})| < |E_{\omega_O}(\text{PEO})|$), and the short C−O bond does not permit the C−H···S contact ($E_{\omega_S} = \infty$). The χ interaction, which was defined for PEO to represent the extra stabilization in the $g^\pm g^\pm g^\pm$ conformations,[3] is of no effect in PEOES ($E_\chi \simeq 0$). Bond conformations (trans fractions) of MEMS, calculated from the ΔG_k values as described previously,[15] are listed in Table 4. As found for PEO[3,4] and PES,[3] the C−O and C−S bonds of PEOES have the trans and gauche preferences, respectively.

Table 3. Conformational Energies (kcal mol^{-1}) of PEOES (MEMS), PEO (DME and Triglyme), and PES (BMTE), Evaluated from Ab Initio MO Calculations[a]

	PEOES		PEO		PES
	MEMS gas	MEMS benzene	DME[b] gas	triglyme[b] gas	BMTE[c] gas
First-Order Interaction					
E_{ρ_O}	1.04	0.94	1.30	1.05	
E_σ	0.50	0.37	0.08	−0.08	0.89
E_{ρ_S}	−0.37	−0.37			−0.41
Second- and Third-Order Interactions					
E_{ω_O}	−0.38	−0.11	−1.02	−1.14	
E_{ω_S}[d]	∞	∞			0.45
E_κ	−0.26	−0.26			−0.19
E_χ	0.08	0.07	−0.42	−0.37	0.50
$E_{\omega'_S}$[e]	0.92	0.93			0.00
S_{conf}[f], cal mol^{-1} deg^{-1}	10.1	10.4	4.8	5.0	5.3

[a] Abbreviations: PEOES, poly(ethylene oxide-*alt*-ethylene sulfide); PEO, poly(ethylene oxide); PES, poly(ethylene sulfide); MEMS, 2-methoxyethyl methyl sulfide; DME, 1,2-dimethoxyethane, $CH_3OCH_2CH_2OCH_3$; triglyme, $CH_3O[CH_2CH_2O]_3CH_3$; BMTE, 1,2-bis(methylthio)ethane, $CH_3SCH_2CH_2SCH_3$. [b] Reference 4. [c] Reference 3. [d] The second-order C−H···S interaction. MEMS does not form $g^\pm g^\mp$ conformations in the C−O/C−C bond pair; therefore, this interaction energy is assumed to be ∞. [e] Determined from a dimeric model compound, $CH_3[SCH_2CH_2OCH_2CH_2]_2SCH_3$. [f] At 25 °C. With respect to the most stable conformation.

Bond dipole moments along the C−O and C−S bonds, m_{C-O} and m_{C-S}, were, respectively, determined as 1.13 and 1.24 D

Table 4. Bond Conformations of MEMS and PEOES

compound	medium	permittivity	temp, °C	p_t^{CO} case III	p_t^{CO} case IV	p_t^{CC} case I	p_t^{CC} case II	p_t^{CS} case V
			MO Calculation					
MEMS	gas	1.0	15		0.83		0.52	0.15
			25		0.82		0.52	0.15
			35		0.82		0.52	0.16
			45		0.81		0.52	0.16
			55		0.80		0.51	0.17
	benzene	2.2	15		0.79		0.56	0.18
			25		0.78		0.55	0.19
			35		0.78		0.55	0.19
			45		0.77		0.55	0.19
			55		0.76		0.54	0.20
PEOES [a]	benzene	2.2	15		0.78		0.53	0.28
			25		0.77		0.53	0.28
			35		0.77		0.52	0.28
			45		0.76		0.52	0.29
			55		0.75		0.52	0.29
			NMR Experiment[b]					
MEMS	C_6D_{12}	2.0	15	0.80	0.75	0.48	0.54	0.14
			25	0.79	0.74	0.47	0.53	0.14
			35	0.78	0.73	0.47	0.52	0.15
			45	0.77	0.72	0.46	0.52	0.15
			55	0.76	0.72	0.45	0.51	0.15
	C_6D_6	2.2	15	0.78	0.74	0.47	0.53	0.20
			25	0.77	0.73	0.47	0.52	0.21
			35	0.76	0.72	0.47	0.52	0.21
			45	0.76	0.71	0.46	0.51	0.21
			55	0.75	0.70	0.45	0.50	0.21
	$CDCl_3$	4.8	15	0.80	0.76	0.48	0.54	0.27
			25	0.79	0.75	0.47	0.53	0.26
			35	0.78	0.73	0.46	0.52	0.26
			45	0.77	0.72	0.44	0.49	0.26
			55	0.76	0.71	0.43	0.49	0.26
	$(CD_3)_2SO$	46.7	15	0.75	0.70	0.45	0.49	0.25
			25	0.74	0.69	0.44	0.47	0.25
			35	0.74	0.68	0.42	0.45	0.26
			45	0.73	0.67	0.41	0.44	0.26
			55	0.72	0.67	0.41	0.44	0.26
	CD_3OD	32.7	15	0.78	0.73	0.40	0.44	0.24
			25	0.77	0.72	0.39	0.42	0.24
			35	0.76	0.71	0.37	0.40	0.25
			45	0.75	0.70	0.35	0.38	0.25
			55	0.74	0.69	0.35	0.38	0.25

[a] By the RIS scheme. [b] For the ^3J_T and ^3J_G values used in each case, see text.

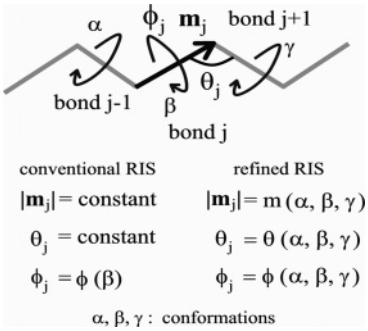

Figure 4. Illustration of the conventional and refined RIS models.

from the MO calculations, μ^{MO}'s.[16] Then, m_{C-C} was assumed to be null. The dipole moments (μ^{BOND}'s) calculated from $m_{C-O} = 1.13$ D, $m_{C-C} = 0.00$, and $m_{C-S} = 1.24$ D are in fairly good agreement with μ^{MO}'s. The m_{C-O} and m_{C-S} values are consistent with those determined previously: $m_{C-O} = 1.18$ D (PEO),[3] 1.17−1.19 D (poly(propylene oxide) and poly(tetramethylene oxide)),[17] and 1.17 D (poly(trimethylene oxide));[6] $m_{C-S} = 1.23$ D (poly(methylene sulfide),[18] 1.22 D (PES),[3] 1.21 D (poly(propylene sulfide)),[19] and 1.22 D (poly(trimethylene sulfide)).[6]

3.2. Refined RIS Scheme. In the RIS scheme, the bond length (bond dipole moment), bond angle, and dihedral angle are multiplied by the statistical weight to be averaged. This operation is performed in the so-called generator matrix G_j (j indicates the bond number or the current bond, and the bond is identified hereafter by the number).[1,2] Their product $G_1G_2\cdots G_n$ (n: number of skeletal bonds) yields the mean-square end-to-end distance or mean-square dipole moment of the polymer. If the statistical weight matrix, U_j, is so defined as to be 9×9, intramolecular interactions, expressed as a function of conformations of bonds $j-2$, $j-1$, and j, are included in U_j. According to the additivity of conformational energies, the U_j matrix is formulated with bonds $\geq j+1$ left out of consideration. On the other hand, the geometrical parameters of bond j depend on conformations of bonds $j-1$ and $j+1$ as well as j, and the effects of distant bonds $\leq j-2$ and $\geq j+2$ may be negligible. In the refined RIS scheme, the generator matrix, $G_{\beta\gamma}$, includes statistical weights related to bonds $j-2$, $j-1$, and j and geometrical parameters for particular β and γ and all α conformations. Here, rotational isomeric states of bonds $j-1$, j, and $j+1$ are denoted as α, β, and γ, respectively (see Figure 4). The $G_{\beta\gamma}$ matrices compose a *supergenerator* matrix Γ_j so

that the product of Γ_j's satisfies the consistency in conformational sequence. The mean-square moment and partition function can be derived from components of the product of all the Γ_j matrices. The details are described below.

In the refined RIS scheme, the mean-square moment $\langle M^2 \rangle$ is given by

$$\langle M^2 \rangle = 2Z^{-1} \sum_{k=1}^{n_{\mathrm{RIS}}} \sum_{o=1}^{n_{\mathrm{RIS}}} \sum_{p=1}^{t_n} g_{5s_1(k-1)+1,\ 5t_n o - p + 1} \tag{1}$$

where n_{RIS} is the number of rotational isomeric states of a skeletal bond (here, $n_{\mathrm{RIS}} = 3$), and Z is the partition function of the polymeric chain, calculated from

$$Z = \sum_{k=1}^{n_{\mathrm{RIS}}} \sum_{o=1}^{n_{\mathrm{RIS}}} \sum_{p=1}^{t_n} g_{5s_1(k-1)+1,\ 5t_n(o-1)+p} \tag{2}$$

with $g_{q,r}$ being the (q, r) element of the product of all Γ_j matrices:

$$(g_{q,r}) = \Gamma_{\mathrm{all}} \equiv \prod_{j=1}^{n} \Gamma_j \tag{3}$$

The statistical weight matrices (U_1 and U_n) of the first and last skeletal bonds have sizes of $s_1 \times t_1$ and $s_n \times t_n$, respectively (here, $s_1 = 3$ and $t_n = 9$, see Appendix). The size of the Γ_{all} matrix is $15s_1 \times 15t_n$. The Γ_j matrix for bond j is composed of nine generator matrices:

$$\Gamma_j = \begin{bmatrix} G_{tt} & G_{tg^+} & G_{tg^-} \\ G_{g^+t} & G_{g^+g^+} & G_{g^+g^-} \\ G_{g^-t} & G_{g^-g^+} & G_{g^-g^-} \end{bmatrix} \tag{4}$$

The rows and columns, respectively, correspond to the rotational isomeric states of bonds j and $j + 1$. The $G_{\beta\gamma}$ matrix of bond j is defined as

$$G_{\beta\gamma} = \begin{bmatrix} U_\beta & [(U_\beta M_\gamma) \otimes R_3] ||T||_\gamma & (1/2) U_\beta (M_\gamma)^2 \\ \mathbf{0} & (U_\beta \otimes I_3) ||T||_\gamma & (U_\beta M_\gamma) \otimes C_3 \\ \mathbf{0} & \mathbf{0} & U_\beta \end{bmatrix} \tag{5}$$

where $\otimes$ stands for direct product. In U_β, the columns of the β state are equal to those of U_j, and other columns are filled with zero; therefore, we have

$$U_j = U_{\mathrm{t}} + U_{\mathrm{g}^+} + U_{\mathrm{g}^-} \tag{6}$$

The moment matrix, M_γ, is defined as

$$M_\gamma = \begin{bmatrix} m_{\mathrm{t}\gamma} & 0 & 0 \\ 0 & m_{\mathrm{g}^+\gamma} & 0 \\ 0 & 0 & m_{\mathrm{g}^-\gamma} \end{bmatrix} \tag{7}$$

for $j = 1$ and 2 or

$$M_\gamma = \begin{bmatrix} m_{\mathrm{tt}\gamma} & & & & & & & & \mathbf{0} \\ & m_{\mathrm{tg}^+\gamma} & & & & & & & \\ & & m_{\mathrm{tg}^-\gamma} & & & & & & \\ & & & m_{\mathrm{g}^+\mathrm{t}\gamma} & & & & & \\ & & & & m_{\mathrm{g}^+\mathrm{g}^+\gamma} & & & & \\ & & & & & m_{\mathrm{g}^+\mathrm{g}^-\gamma} & & & \\ & & & & & & m_{\mathrm{g}^-\mathrm{t}\gamma} & & \\ & & & & & & & m_{\mathrm{g}^-\mathrm{g}^+\gamma} & \\ \mathbf{0} & & & & & & & & m_{\mathrm{g}^-\mathrm{g}^-\gamma} \end{bmatrix} \tag{8}$$

for $j \geq 3$. Here, $m_{\alpha\beta\gamma}$ is either bond length or bond dipole moment. Inasmuch as $M_\gamma = \mathrm{diag}(\cdots m_{\alpha\beta\gamma} \cdots)$, we have $(M_\gamma)^2 = \mathrm{diag}(\cdots {m_{\alpha\beta\gamma}}^2 \cdots)$. The R_3, I_3, and C_3 are row, column, identity matrices of size 3, respectively:

$$R_3 = [1 \ \ 0 \ \ 0] \tag{9}$$

$$C_3 = \begin{bmatrix} 1 \\ 0 \\ 0 \end{bmatrix} \tag{10}$$

and

$$I_3 = \begin{bmatrix} 1 & 0 & 0 \\ 0 & 1 & 0 \\ 0 & 0 & 1 \end{bmatrix} \tag{11}$$

The $||T||_\gamma$ matrix is defined as

$$||T||_\gamma = \begin{bmatrix} T_{\mathrm{t}\gamma} & & \mathbf{0} \\ & T_{\mathrm{g}^+\gamma} & \\ \mathbf{0} & & T_{\mathrm{g}^-\gamma} \end{bmatrix} \tag{12}$$

for $j = 1$ and 2 or

$$||T||_\gamma = \begin{bmatrix} T_{\mathrm{tt}\gamma} & & & & & & & & \mathbf{0} \\ & T_{\mathrm{tg}^+\gamma} & & & & & & & \\ & & T_{\mathrm{tg}^-\gamma} & & & & & & \\ & & & T_{\mathrm{g}^+\mathrm{t}\gamma} & & & & & \\ & & & & T_{\mathrm{g}^+\mathrm{g}^+\gamma} & & & & \\ & & & & & T_{\mathrm{g}^+\mathrm{g}^-\gamma} & & & \\ & & & & & & T_{\mathrm{g}^-\mathrm{t}\gamma} & & \\ & & & & & & & T_{\mathrm{g}^-\mathrm{g}^+\gamma} & \\ \mathbf{0} & & & & & & & & T_{\mathrm{g}^-\mathrm{g}^-\gamma} \end{bmatrix} \tag{13}$$

for $j \geq 3$. The $T_{\beta\gamma}$ ($j \leq 2$) and $T_{\alpha\beta\gamma}$ ($j \geq 3$) matrices transform a vector from the j th to $(j - 1)$th frame of reference. The $T_{\alpha\beta\gamma}$ matrix is expressed as

$$T_{\alpha\beta\gamma} = \begin{bmatrix} -\cos\theta_{\alpha\beta\gamma} & \sin\theta_{\alpha\beta\gamma} & 0 \\ \sin\theta_{\alpha\beta\gamma}\cos\phi_{\alpha\beta\gamma} & \cos\theta_{\alpha\beta\gamma}\cos\phi_{\alpha\beta\gamma} & \sin\phi_{\alpha\beta\gamma} \\ \sin\theta_{\alpha\beta\gamma}\sin\phi_{\alpha\beta\gamma} & \cos\theta_{\alpha\beta\gamma}\sin\phi_{\alpha\beta\gamma} & -\cos\phi_{\alpha\beta\gamma} \end{bmatrix} \tag{14}$$

where $\theta_{\alpha\beta\gamma}$ is the bond angle, and $\phi_{\alpha\beta\gamma}$ is the dihedral angle for the β state of bond j with bonds $j - 1$ and $j + 1$ being in the α and γ states, respectively. The $T_{\beta\gamma}$ matrix is similarly defined. The sizes of the block matrices of $G_{\beta\gamma}$ are

$$\begin{bmatrix} s \times t & s \times 3t & s \times t \\ 3s \times t & 3s \times 3t & 3s \times t \\ s \times t & s \times 3t & s \times t \end{bmatrix} \tag{15}$$

where (s, t) corresponds to the size of U_j. For the terminal bonds ($j = 1$ and n), the $G_{\beta\gamma}$ and Γ_j matrices can be similarly prepared from U_1 and U_n. If the Γ_j matrices of the repeating unit are combined into one, eq 3 can be rewritten as

$$\Gamma_{\text{all}} = \Gamma_1 H_1 (\prod_{i=2}^{x} H_i) \Gamma_n \tag{16}$$

where i is the unit number, and x is the degree of polymerization. For PEOES, the H matrices are given as

$$H_1 \equiv \Gamma_2 \Gamma_3 \cdots \Gamma_7 \tag{17}$$

and

$$H_i \equiv \Gamma_a \Gamma_b \cdots \Gamma_f \tag{18}$$

The computation of eq 16 is much more efficient than that of eq 3.

The characteristic ratio, $\langle r^2 \rangle_0 / nl^2$, and dipole moment ratio, $\langle \mu^2 \rangle / nm^2$, can be calculated from

$$\langle r^2 \rangle_0 / nl^2 \text{ or } \langle \mu^2 \rangle / nm^2 = \langle M^2 \rangle \, [\sum_{j=1}^{n} (\bar{m}_j)^2]^{-1} \tag{19}$$

where $\bar{m}_j$ is the mean bond length or mean bond dipole moment, given by

$$\bar{m}_j = \sum_{\alpha} \sum_{\beta} \sum_{\gamma} m_{\alpha\beta\gamma, j} \, p_{\alpha\beta\gamma, j} \tag{20}$$

Here, $p_{\alpha\beta\gamma,j}$ is the probability of the $\alpha\beta\gamma$ conformation for bond j, calculated as in the conventional RIS scheme.[1,2] The bond angle and dihedral angle are also averaged similarly:

$$\bar{\theta}_j = \sum_{\alpha} \sum_{\beta} \sum_{\gamma} \theta_{\alpha\beta\gamma, j} \, p_{\alpha\beta\gamma, j} \tag{21}$$

and

$$\bar{\phi}_{\beta, j} = \sum_{\alpha} \sum_{\gamma} \phi_{\alpha\beta\gamma, j} \, p_{\alpha\beta\gamma, j} \, (\sum_{\alpha} \sum_{\gamma} p_{\alpha\beta\gamma, j})^{-1} \tag{22}$$

These averages, calculated from the statistical weight matrices, depend on temperature. Other physical properties, for example, the scattering of radiation and optical anisotropy and activity, having been related to the conventional RIS model,[1,2] may also be formulated under the refined RIS scheme.

3.3. Configurational Properties of PEOES. The geometrical parameters required for the refined RIS calculations for PEOES were obtained from EEES as shown in Table 1. The bond dipole moments were treated as constants, because there was no sufficient information to investigate the conformation dependence of the m values. The dipole moment ratios and characteristic ratios of PEOES, calculated as explained in the preceding section, are plotted in Figure 5 against the reciprocal (x^{-1}) of degree of polymerization. Table 5 shows the $\langle r^2 \rangle_0 / nl^2$ and $\langle \mu^2 \rangle / nm^2$ values and their temperature coefficients at $x = 100$ and ∞. The geometrical parameters were averaged according to eqs 20−22 (Table 6). Compared in Table 3 are the configurational entropies, S_{conf}'s, of PEOES, PEO, and PES, calculated with[6,20,21]

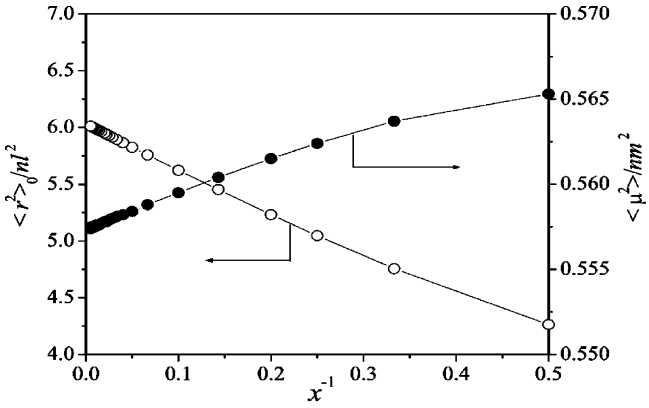

Figure 5. Characteristic ratio ($\langle r^2 \rangle_0 / nl^2$) and dipole moment ratio ($\langle \mu^2 \rangle / nm^2$) of PEOES as a function of the reciprocal (x^{-1}) of degree of polymerization.

$$S_{\text{conf}} = R\left(\ln z + T \frac{d \ln z}{dT}\right) \tag{23}$$

from the conformational energies given there. Here, z is the partition function per mole of monomer:

$$z = Z^{1/x} \tag{24}$$

The repeating unit of PEOES has six skeletal bonds, and those of PEO and PES have three; accordingly, the three polymers have close $S_{\text{conf}}/n_{\text{unit}}$ values, where n_{unit} is the number of skeletal bonds in the repeating unit. The melting point (T_m in K) is related to the enthalpy (ΔH_u) and entropy (ΔS_u) of fusion by

$$T_m = \frac{\Delta H_u}{\Delta S_u} \tag{25}$$

The configurational entropy accounts for 80−90% of ΔS_u.[6] The melting points of PEOES, PEO, and PES are 45−48, 66−69, and 215−220 °C, respectively.[6,22] Despite the similar $S_{\text{conf}}/n_{\text{unit}}$ values, only PES exhibits the extraordinarily high melting point. This stems from a large ΔH_u term due to dipole−dipole interactions in the PES crystal.[6]

3.4. ^{1}H NMR. Figure 6 shows ^{1}H NMR spectra observed from methylene protons of MEMS. Two vicinal coupling constants, $^3J_{HH}$ ($= {}^3J_{AB} = {}^3J_{A'B'}$) and $^3J'_{HH}$ ($= {}^3J_{AB'} = {}^3J_{A'B}$), derived from the gNMR simulations,[13] are given in Table 7. The coupling constants are expressed as a function of trans (p_t^{CC}) and gauche (p_g^{CC}) fractions of the C−C bond:

$${}^3J_{HH} = {}^3J_G^{HH} \, p_t^{CC} + \frac{{}^3J'_T{}^{HH} + {}^3J''_G{}^{HH}}{2} p_g^{CC} \tag{26}$$

and

$${}^3J'_{HH} = {}^3J_T^{HH} \, p_t^{CC} + \frac{{}^3J'_G{}^{HH} + {}^3J'''_G{}^{HH}}{2} p_g^{CC} \tag{27}$$

The $^3J_T^{HH}$'s and $^3J_G^{HH}$ values (Figure 2) were evaluated by two methods: case I, NMR experiments for MOT (Table 8); case II, MO calculations for MEMS itself (Table 9). Figure 7 shows an example of the observed and calculated ^{1}H NMR spectra of MOT. The p_t^{CC} and p_g^{CC} values derived from the above equations were divided by their sum to satisfy $p_t^{CC} + p_g^{CC} = 1$. The results of cases I and II somewhat differ from each other;

Table 5. Calculated and Observed Configurational Properties of PEOES

	x	$\langle\mu^2\rangle/nm^2$	10^3 d(ln $\langle\mu^2\rangle$)/dT (K^{-1})	$\langle r^2\rangle_0/nl^2$	10^3 d(ln $\langle r^2\rangle_0$)/dT (K^{-1})
calcd[a]					
refined RIS[b]	100	0.56	1.1	6.0	0.22
	∞	0.56		6.0	
conventional RIS [c]	100	0.54	1.0	5.2	−0.09
	∞	0.54		5.3	
obsd	ca. 100[d]	0.57[e]	1.6	*f*	*f*

[a] From the conformational energies of PEOES (MEMS) in benzene (Table 3). [b] Using the geometrical parameters shown in Table 1. [c] Using the averaged geometrical parameters (Table 6). [d] In the dipole moment measurements, two samples (number-average molecular weight = 8×10^3 and 13×10^3) were used.[22,24] [e] Recalculated with $m_{C-O} = 1.13$, $m_{C-C} = 0.00$, and $m_{C-S} = 1.24$ D. [f] No experimental data are available.

Table 6. Averaged Geometrical Parameters for PEOES[a]

Bond Length, Å	
$\bar{l}_{CO}$	1.416
$\bar{l}_{CC}$	1.526
$\bar{l}_{CS}$	1.837
Bond Angle, deg	
$\bar{\theta}_{COC}$	113.7
$\bar{\theta}_{OCC}$	109.5
$\bar{\theta}_{CCS}$	113.4
$\bar{\theta}_{CSC}$	101.4
Dihedral Angle,[b] deg	
$\bar{\phi}_{g\pm}$(C−O)	±101.1
$\bar{\phi}_{g\pm}$(C−C)	±113.9
$\bar{\phi}_{g\pm}$(C−S)	±97.9

[a] At 25 °C. Obtained for each type with eqs 20−22 from the geometrical parameters shown in Table 1, for example, $\bar{\theta}_{COC} = \sum_{COC}\bar{\theta}_j$/(number of ∠COC's). [b] $\bar{\phi}_t$(C−O) = $\bar{\phi}_t$(C−C) = $\bar{\phi}_t$(C−S) = 0°.

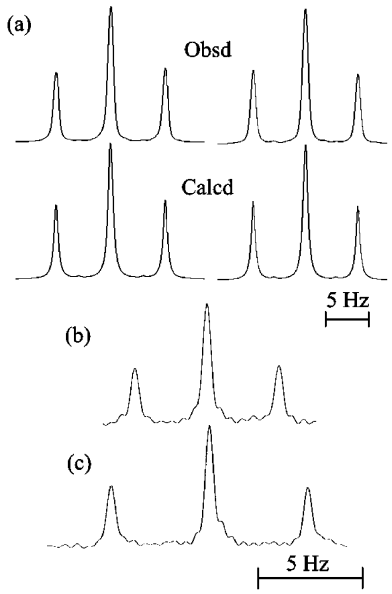

Figure 6. (a) ^{1}H NMR spectra of methylene protons, A and A′ (left) and B and B′ (right), of MEMS dissolved in C_6D_6 at 25 °C. ^{13}C NMR spectra of methyl protons, (b) CH_3O- and (c) CH_3S-, of MEMS in CD_3OD at 35 °C.

the case II data are closer to the MO calculations. The trans fraction decreases with an increase in temperature or solvent polarity.

3.5. ^{13}C NMR. Figure 6 shows observed ^{13}C NMR spectra of methyl carbons of MEMS. The triplet directly gives the vicinal coupling ($^3J_{CH}$) of $^{13}CH_3-O-CH_2$ or $^{13}CH_3-S-CH_2$. The $^3J_{CH}$ values for the five solutions are listed in Table 7. The observed $^3J_{CH}$ value is expressed as

$$^3J_{CH} = {}^3J_G^{CH}\, p_t^{CX} + \frac{{}^3J_T'^{CH} + {}^3J_G'^{CH}}{2} p_g^{CX} \qquad (28)$$

Table 7. Observed Vicinal ^{1}H−^{1}H and ^{13}C−^{1}H Coupling Constants of MEMS[a]

				$^3J_{CH}$	
solvent	temp, °C	$^3J_{HH}$	$^3J'_{HH}$	C−O	C−S
C_6D_{12}	15	6.03	7.84	3.23	5.23
	25	6.08	7.76	3.29	5.21
	35	6.10	7.70	3.33	5.19
	45	6.13	7.65	3.38	5.18
	55	6.18	7.60	3.42	5.16
C_6D_6	15	6.00	7.60	3.31	4.98
	25	6.01	7.58	3.37	4.96
	35	6.02	7.55	3.42	4.96
	45	6.06	7.49	3.46	4.95
	55	6.10	7.44	3.51	4.94
$CDCl_3$	15	5.79	7.51	3.22	4.73
	25	5.85	7.45	3.27	4.75
	35	5.92	7.41	3.33	4.75
	45	6.07	7.29	3.39	4.76
	55	6.10	7.26	3.44	4.75
$(CD_3)_2SO$	15	6.11	7.26	3.48	4.79
	25	6.20	7.19	3.54	4.79
	35	6.30	7.10	3.58	4.77
	45	6.31	7.01	3.63	4.77
	55	6.33	6.96	3.67	4.76
CD_3OD	15	6.29	6.95	3.35	4.84
	25	6.41	6.86	3.40	4.83
	35	6.49	6.73	3.45	4.80
	45	6.61	6.61	3.50	4.78
	55	6.60	6.60	3.55	4.78

[a] In Hz.

Table 8. Vicinal ^{1}H−^{1}H Coupling Constants of MOT[a]

solvent	$^3J_T^{HH}$	$^3J_G'^{HH}$	$^3J_G''^{HH}$	$^3J_G'''^{HH}$	$^3J_G^{HH}$
C_6D_{12}	10.57	2.21	3.30	3.24	2.92
C_6D_6	10.61	2.18	3.40	3.21	2.93
$CDCl_3$	10.59	2.45	3.20	3.08	2.91
$(CD_3)_2SO$	10.39	2.22	3.49	3.17	2.96
CD_3OD	10.60	2.23	3.26	3.16	2.88

[a] In Hz. At 25 °C. For definitions of the coupling constants, see Figure 7. $^3J_T^{HH} = {}^3J_T'^{HH}$ and $^3J_G^{HH} = ({}^3J_G'^{HH} + {}^3J_G''^{HH} + {}^3J_G'''^{HH})/3$.

where $^3J_T'^{CH}$ and $^3J_G^{CH}$'s are defined in Figure 2, and p_t^{CX} and p_g^{CX} are trans and gauche fractions of the C−X (X = O or S) bond, respectively. For X = O, two sets of $^3J^{CH}$'s were adopted: case III, those optimized for DME and PEO, namely, $^3J_G^{CH} = 2.0$ Hz and $^3J_T'^{CH} + {}^3J_G'^{CH} = 16.0$ Hz;[23] case IV, the MO calculations for MEMS (Table 9). The p_t^{CO} values thus derived are listed in Table 4. For X = S, the $^3J_T^{CH}$ and $^3J_G^{CH}$ values of 2-methyl-1,3,5-trithiane[18] were tentatively used on the assumption that $^3J_G^{CH} = {}^3J_G'^{CH}$. For example, substitution of $^3J_T'^{CH} = 7.13$, $^3J_G^{CH} = {}^3J_G'^{CH} = 2.62$, and $^3J_{CH} = 4.98$ Hz (C_6D_6 at 15 °C) into eq 28 yielded $p_t^{CS} = -0.05$. The MO calculations show a large difference between $^3J_G^{CH}$ (1.91 Hz) and $^3J_G'^{CH}$ (4.21 Hz); therefore, the assumption of $^3J_G^{CH} = {}^3J_G'^{CH}$ gave rise to the negative p_t^{CS} value. For X = S, therefore, the calculated $^3J^{CH}$ values (Table 9) were used (case V). The p_t^{CS} values are also listed in Table 4.

Table 9. Vicinal Coupling Constants of MEMS, Obtained from MO Calculations[a]

CH_3-O-CH_2-		O-CH_2-CH_2-S		-CH_2-S-CH_3	
		$^3J_T^{HH}$	10.80		
$^3J_G^{CH}$	1.99	$^3J_G^{HH}$	4.50	$^3J_G^{CH}$	1.91
$^3J'^{CH}_T$	9.04	$^3J'^{HH}_T$	10.75	$^3J'^{CH}_T$	7.29
$^3J'^{CH}_G$	5.00	$^3J'^{HH}_G$	2.09	$^3J'^{CH}_G$	4.21
		$^3J''^{HH}_G$	2.34		
		$^3J'''^{HH}_G$	3.21		

[a] In Hz. At the B3LYP/6-311++G(3df, 3pd)//B3LYP/6-31G(d) level. For definitions of the coupling constants, see Figure 2.

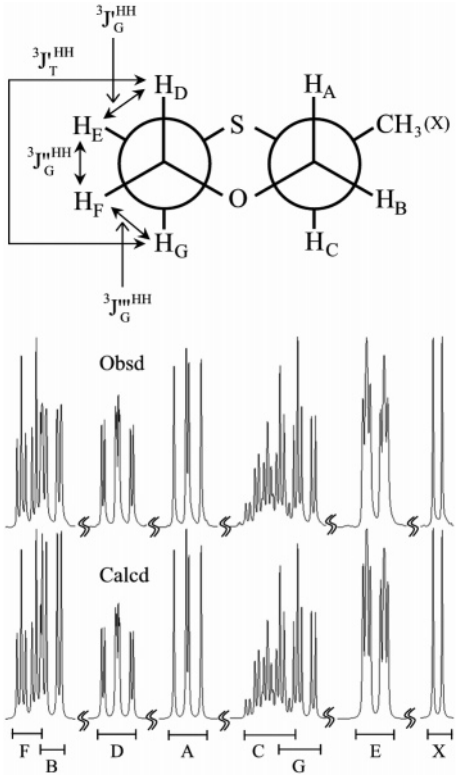

Figure 7. ^{1}H NMR spectra of 3-methyl-1,4-oxathiane (MOT) dissolved in C_6D_{12} at 25 °C. As shown, the peaks were assigned. The NMR parameters were determined as follows (δ in ppm and J in Hz): $\delta_A = 3.24$, $\delta_B = 3.93$, $\delta_C = 2.83$, $\delta_D = 3.53$, $\delta_E = 2.29$, $\delta_F = 3.97$, $\delta_G = 2.79$, $\delta_X = 1.06$, $^2J_{AB} = -11.42$, $^3J_{AC} = 9.39$, $^3J_{BC} = 3.07$, $^4J_{BF} = 0.35$, $^3J_{DE} = 2.21$, $^2J_{DF} = -11.47$, $^3J_{DG} = 10.57$, $^3J_{EF} = 3.30$, $^2J_{EG} = -13.49$, $^3J_{FG} = 3.24$, $^3J_{CX} = 6.95$.

4. Discussion

4.1. Comparison between Theory and Experiment. The bond conformations (Table 4) of MEMS and PEOES and the dipole moment ratio, characteristic ratio, and their temperature coefficients (Table 5) of PEOES were calculated by the refined RIS scheme using the conformational energies (Table 3) and geometrical parameters (Table 1) obtained from the MO computations. Thus far, the treatment was thoroughly theoretical; the only empirical factor, used in the MO theory, was the permittivity ($\epsilon_r = 2.247$) of benzene. The structural and energy data on MEMS, the moiety of the repeating unit of PEOES, were applied to the refined RIS computations, and, consequently, the canonical ensemble averages on PEOES were given as the characteristic ratio, dipole moment ratio, configurational entropy, and so on. On the other hand, the analyses of the NMR and dipole moment experiments needed the aid of the MO calculations in evaluating $^3J^{HH}$'s, $^3J^{CH}$'s, and m's. As shown in Tables 4 and 5, the theoretical and experimental values of the bond conformations, dipole moment ratio, and its temperature coefficient[22,24] are in close agreement; the configurational properties of PEOES in benzene have been exactly reproduced only from quantum chemistry and statistical mechanics. Between the repeating units, PEOES has a symmetry plane and a 2-fold symmetry axis; therefore, the dipole moment observed from PEOES is always free from the excluded volume effect.[25,26] A slight discrepancy in $d(\ln \langle\mu^2\rangle)/dT$ is seen between theory and experiment; however, this result should be satisfactory, because the conventional RIS scheme has often reproduced the experimental temperature coefficients of $\langle\mu\rangle/nm^2$ and $\langle r^2\rangle_0/nl^2$ qualitatively rather than quantitatively. So far, no one has synthesized PEOES of molecular weights enough to yield the radius of gyration by light scattering or viscometry, and hence the characteristic ratio at the Θ point remains unknown. The intrinsic viscosity $[\eta]_\Theta$ of an unperturbed polymer is related to the mean-square end-to-end distance by the Flory-Fox equation:[2,27]

$$[\eta]_\Theta = \Phi_0 \left(\frac{\langle r^2\rangle_0}{M}\right)^{3/2} M^{1/2} \tag{29}$$

where Φ_0 is the viscosity coefficient at the Θ point, and M is the molecular weight. Accordingly, if the Θ condition is found, the present calculations would yield the viscosity as well as the unperturbed dimension. It has been established that molten inert polymers[28] are unperturbed.[29] The calculations here also provide information on the polymer melt. For dilute polymer solutions, the spatial configuration of the polymer has been determined from light scattering and viscosity measurements.[30] For polymer melts, the radii of gyration have been estimated from neutron scattering experiments using deuterium labeled samples.[31] Such laborious experiments may be partly replaced by the theoretical treatments.

4.2. Refined RIS Model. The refined RIS model includes details of the chemical structure, namely, atom, bond length, bond angle, dihedral angle, and intramolecular interaction, and it needs no ad hoc parameter. Within the framework of the RIS approximation, this model represents the polymeric chain as precisely as possible. The exact agreement between theory and experiment indicates that the intramolecular interactions are in actual existence as reported here. Even simple models such as the freely jointed chain and the Gaussian coil can provide the molecular weight dependence of the radius of gyration in the Θ state.[1,32] However, this study has demonstrated that the elaborate treatment is indispensable for the rigorous expression of the unperturbed chain. With the weight-averaged geometrical parameters (Table 6), the conventional RIS scheme also affords the dipole moment and its temperature coefficient close to the observations (Table 5). However, the two RIS models have made a difference of 13 % in $\langle r^2\rangle_0/nl^2$ and given the temperature coefficients of different signs. For polymers forming intramolecular attractions and hence distorting the molecular geometry, in particular, the refined RIS scheme must be more suitable, and its validity and advantages will be further examined through its applications to other polymers.

4.3. Solvent Effects. The MO calculations using the IEF-PCM model[9,10] closely reproduced the experimental bond conformations of MEMS dissolved in benzene. In a previous study,[15] we applied the Onsager model,[33,34] which assumes the solute as a sphere, to 1,2-dimethoxypropane, a model compound of poly(propylene oxide), calculated the conformational energies including the solvent effect, and compared the calculations with

NMR experiments, but the results were not satisfactory. For this decade, the solvation model has been improved. However, there remain still more complicated solvent effects to be tackled. Intramolecular (C−H)···O and N−H···N attractions, formed in polyethers and polyimines, respectively, are switched to specific polymer−solvent interactions.[3,4,14,15,35] In aqueous solutions, ionized polymers, for example, cationic poly(ethylene imine), are coupled with hydrated counterions, and the solution properties depend largely on pH.[36,37] It is uncertain whether the Θ states of these systems can be considered to be similar to those of inert systems[28] (e.g., polystyrene in cyclohexane at 34.5°C)[38] that are ideal objects of the Flory−Huggins theory.[39] The former systems are subject to van der Waals forces, electrostatic forces, and hydrogen-bond-like weak attractions, and the latter are dominated by van der Waals interactions.

4.4. Nature of the (C−H)···O Attraction. Of the conformational energies shown in Table 3, the ω_O interaction, corresponding to the (C−H)···O attraction, seems to be selectively affected by the solvation: −0.38 (in the gas phase) → −0.11 kcal mol^{-1} (in benzene). The σ interaction energy is somewhat reduced, but other energies are unchanged. Similar tendencies have been found for PEO.[3,4,40,41,42] The (C−H)···O interaction has often been termed a weak hydrogen bond. From the word "bond", we feel the interaction to be static and stable. When it is found in molecular crystals and supermolecules,[43] this impression may be reasonable. However, this study has dealt with the polymers and model compounds in rapid molecular motions. In general, MO calculations are based on the Born−Oppenheimer approximation,[44] which assures that the electronic state can be treated separately from nuclear motions; in a molecule, the electrons can promptly adjust themselves to any given nuclear arrangement. Accordingly, the (C−H)···O attraction is formed only when the related atoms come close to each other. In MEMS, for example, the attraction appears only in the $tg^{\pm}g^{\mp}$ conformations (see Figure 3a). The transitions from these to other conformations extinguish the (C−H)···O interaction. Such a transient interaction, being far from a chemical bond, may be preferably termed an attraction. So far, we have found weak attractions such as (C−H)···O, N−H···N, and N−H···O and elucidated how they determine the conformations, configurations, secondary structures, crystal structures, physical properties, and functions of the polymers.[3−5,14,15,17,35,45] It is probably organisms that best utilize such weak interactions on earth. We think that the interpretation of vital phenomena in terms of weak attractions will become one of the more important subjects of chemistry.

5. Conclusion

The refined RIS scheme, a statistical mechanics technique for polymers, including the dependence of geometrical parameters as well as interaction energies on conformations of the current and neighboring bonds, has been developed and applied to conformational analysis of PEOES with the geometrical and energy parameters determined from ab initio MO calculations for its model compounds. This study has suggested the possibility that conformational characteristics and configurational properties of polymers in nonpolar solvents and in the melt can be elucidated by the purely theoretical treatment and adduced definite evidence for Flory's idea of the unperturbed polymer:[2,29,39] without the excluded volume effect, the polymer configuration should be determined only from short-range intramolecular interactions. Computational polymer science is going to enable us to derive reliable data on structures and properties, elucidate the structure−property relationships, and design new polymers.

Appendix A.

Statistical Weight Matrices of MEMS (PEOES). Statistical weight matrices, U_j, of MEMS and PEOES were formulated according to the 9 × 9 scheme:

$$U_1 = \begin{bmatrix} 1 & 1 & 1 \\ 0 & 0 & 0 \\ 0 & 0 & 0 \end{bmatrix} \tag{A1}$$

$$U_2 = \begin{bmatrix} 1 & \rho_O & \rho_O \\ 0 & 0 & 0 \\ 0 & 0 & 0 \end{bmatrix} \tag{A2}$$

$$U_3 = \begin{bmatrix} 1 & \sigma & \sigma & 0 & 0 & 0 & 0 & 0 & 0 \\ 0 & 0 & 0 & 1 & \sigma & \sigma\omega_S & 0 & 0 & 0 \\ 0 & 0 & 0 & 0 & 0 & 0 & 1 & \sigma\omega_S & \sigma \end{bmatrix} \tag{A3}$$

$$U_4 = \begin{bmatrix} 1 & \rho_S & \rho_S & 0 & 0 & 0 & 0 & 0 & 0 \\ 0 & 0 & 0 & 1 & \rho_S & \rho_S\omega_O & 0 & 0 & 0 \\ 0 & 0 & 0 & 0 & 0 & 0 & 1 & \rho_S\omega_O & \rho_S \\ 1 & \rho_S & \rho_S\kappa & 0 & 0 & 0 & 0 & 0 & 0 \\ 0 & 0 & 0 & 1 & \rho_S\chi & \rho_S\omega_O & 0 & 0 & 0 \\ 0 & 0 & 0 & 0 & 0 & 0 & 1 & 0 & \rho_S \\ 1 & \rho_S\kappa & \rho_S & 0 & 0 & 0 & 0 & 0 & 0 \\ 0 & 0 & 0 & 1 & \rho_S & 0 & 0 & 0 & 0 \\ 0 & 0 & 0 & 0 & 0 & 0 & 1 & \rho_S\omega_O & \rho_S\chi \end{bmatrix} \tag{A4}$$

$$U_5 = \begin{bmatrix} 1 & \rho_S & \rho_S & 0 & 0 & 0 & 0 & 0 & 0 \\ 0 & 0 & 0 & 1 & \rho_S & \rho_S\omega'_S & 0 & 0 & 0 \\ 0 & 0 & 0 & 0 & 0 & 0 & 1 & \rho_S\omega'_S & \rho_S \\ 1 & \rho_S & \rho_S & 0 & 0 & 0 & 0 & 0 & 0 \\ 0 & 0 & 0 & 1 & \rho_S & \rho_S\omega'_S & 0 & 0 & 0 \\ 0 & 0 & 0 & 0 & 0 & 0 & 1 & 0 & \rho_S \\ 1 & \rho_S & \rho_S & 0 & 0 & 0 & 0 & 0 & 0 \\ 0 & 0 & 0 & 1 & \rho_S & 0 & 0 & 0 & 0 \\ 0 & 0 & 0 & 0 & 0 & 0 & 1 & \rho_S\omega'_S & \rho_S \end{bmatrix} \tag{A5}$$

$$U_6 = \begin{bmatrix} 1 & \sigma & \sigma & 0 & 0 & 0 & 0 & 0 & 0 \\ 0 & 0 & 0 & 1 & \sigma & \sigma\omega_O & 0 & 0 & 0 \\ 0 & 0 & 0 & 0 & 0 & 0 & 1 & \sigma\omega_O & \sigma \\ 1 & \sigma & \sigma & 0 & 0 & 0 & 0 & 0 & 0 \\ 0 & 0 & 0 & 1 & \sigma & \sigma\omega_O & 0 & 0 & 0 \\ 0 & 0 & 0 & 0 & 0 & 0 & 1 & 0 & \sigma \\ 1 & \sigma & \sigma & 0 & 0 & 0 & 0 & 0 & 0 \\ 0 & 0 & 0 & 1 & \sigma & 0 & 0 & 0 & 0 \\ 0 & 0 & 0 & 0 & 0 & 0 & 1 & \sigma\omega_O & \sigma \end{bmatrix} \tag{A6}$$

$$U_7 = \begin{bmatrix} 1 & \rho_O & \rho_O & 0 & 0 & 0 & 0 & 0 & 0 \\ 0 & 0 & 0 & 1 & \rho_O & \rho_O\omega_S & 0 & 0 & 0 \\ 0 & 0 & 0 & 0 & 0 & 0 & 1 & \rho_O\omega_S & \rho_O \\ 1 & \rho_O & \rho_O\kappa & 0 & 0 & 0 & 0 & 0 & 0 \\ 0 & 0 & 0 & 1 & \rho_O\chi & \rho_O\omega_S & 0 & 0 & 0 \\ 0 & 0 & 0 & 0 & 0 & 0 & 1 & 0 & \rho_O \\ 1 & \rho_O\kappa & \rho_O & 0 & 0 & 0 & 0 & 0 & 0 \\ 0 & 0 & 0 & 1 & \rho_O & 0 & 0 & 0 & 0 \\ 0 & 0 & 0 & 0 & 0 & 0 & 1 & \rho_O\omega_S & \rho_O\chi \end{bmatrix} \tag{A7}$$

$$U_a = \begin{bmatrix} 1 & \rho_O & \rho_O & 0 & 0 & 0 & 0 & 0 & 0 \\ 0 & 0 & 0 & 1 & \rho_O & \rho_O\omega'_O & 0 & 0 & 0 \\ 0 & 0 & 0 & 0 & 0 & 0 & 1 & \rho_O\omega'_O & \rho_O \\ 1 & \rho_O & \rho_O & 0 & 0 & 0 & 0 & 0 & 0 \\ 0 & 0 & 0 & 1 & \rho_O & \rho_O\omega'_O & 0 & 0 & 0 \\ 0 & 0 & 0 & 0 & 0 & 0 & 1 & 0 & \rho_O \\ 1 & \rho_O & \rho_O & 0 & 0 & 0 & 0 & 0 & 0 \\ 0 & 0 & 0 & 1 & \rho_O & 0 & 0 & 0 & 0 \\ 0 & 0 & 0 & 0 & 0 & 0 & 1 & \rho_O\omega'_O & \rho_O \end{bmatrix} \quad \text{(A8)}$$

$$U_b = \begin{bmatrix} 1 & \sigma & \sigma & 0 & 0 & 0 & 0 & 0 & 0 \\ 0 & 0 & 0 & 1 & \sigma & \sigma\omega_S & 0 & 0 & 0 \\ 0 & 0 & 0 & 0 & 0 & 0 & 1 & \sigma\omega_S & \sigma \\ 1 & \sigma & \sigma & 0 & 0 & 0 & 0 & 0 & 0 \\ 0 & 0 & 0 & 1 & \sigma & \sigma\omega_S & 0 & 0 & 0 \\ 0 & 0 & 0 & 0 & 0 & 0 & 1 & 0 & \sigma \\ 1 & \sigma & \sigma & 0 & 0 & 0 & 0 & 0 & 0 \\ 0 & 0 & 0 & 1 & \sigma & 0 & 0 & 0 & 0 \\ 0 & 0 & 0 & 0 & 0 & 0 & 1 & \sigma\omega_S & \sigma \end{bmatrix} \quad \text{(A9)}$$

and

$$U_n = \begin{bmatrix} 1 & 1 & 1 & 0 & 0 & 0 & 0 & 0 & 0 \\ 0 & 0 & 0 & 1 & 1 & 1 & 0 & 0 & 0 \\ 0 & 0 & 0 & 0 & 0 & 0 & 1 & 1 & 1 \\ 1 & 1 & 1 & 0 & 0 & 0 & 0 & 0 & 0 \\ 0 & 0 & 0 & 1 & 1 & 1 & 0 & 0 & 0 \\ 0 & 0 & 0 & 0 & 0 & 0 & 1 & 1 & 1 \\ 1 & 1 & 1 & 0 & 0 & 0 & 0 & 0 & 0 \\ 0 & 0 & 0 & 1 & 1 & 1 & 0 & 0 & 0 \\ 0 & 0 & 0 & 0 & 0 & 0 & 1 & 1 & 1 \end{bmatrix} \quad \text{(A10)}$$

The other U_j matrices can be derived from $U_c = U_4$, $U_d = U_5$, $U_e = U_6$, and $U_f = U_7$.

Acknowledgment. This work was partly supported by the Asahi Glass Foundation and a Grant-in-Aid for Scientific Research (B) (18350112) from the Japan Society for the Promotion of Science.

References and Notes

(1) Mattice, W. L.; Suter, U. W. *Conformational Theory of Large Molecules: The Rotational Isomeric State Model in Macromolecular Systems*; Wiley & Sons: New York, 1994.

(2) Flory, P. J. *Statistical Mechanics of Chain Molecules*; Wiley & Sons: New York, 1969.

(3) Sasanuma, Y.; Ohta, H.; Touma, I.; Matoba, H.; Hayashi, Y.; Kaito, A. *Macromolecules* **2002**, *35*, 3748.

(4) Sasanuma, Y.; Sugita, K. *Polym. J.* **2006**, *38*, 983.

(5) Sasanuma, Y. Intramolecular Interactions of Polyethers and Polysulfides, Investigated by NMR, Ab Initio Molecular Orbital Calculations, and Rotational Isomeric State Scheme: An Advanced Analysis of NMR Data. In *Annual Reports on NMR Spectroscopy*; Webb, G. A., Ed.; Academic Press: New York, 2003; Vol. 49, Chapter 5.

(6) Sasanuma, Y.; Watanabe, A. *Macromolecules* **2006**, *39*, 1646.

(7) Frisch, M. J.; Trucks, G. W.; Schlegel, H. B.; Scuseria, G. E.; Robb, M. A.; Cheeseman, J. R.; Montgomery, Jr. J. A.; Vreven, T.; Kudin, K. N.; Burant, J. C.; Millam, J. M.; Iyengar, S. S.; Tomasi, J.; Barone, V.; Mennucci, B.; Cossi, M.; Scalmani, G.; Rega, N.; Petersson, G. A.; Nakatsuji, H.; Hada, M.; Ehara, M.; Toyota, K.; Fukuda, R.; Hasegawa, J.; Ishida, M.; Nakajima, T.; Honda, Y.; Kitao, O.; Nakai, H.; Klene, M.; Li, X.; Knox, J. E.; Hratchian, H. P.; Cross, J. B.; Bakken, V.; Adamo, C.; Jaramillo, J.; Gomperts, R.; Stratmann, R. E.; Yazyev, O.; Austin, A. J.; Cammi, R.; Pomelli, C.; Ochterski, J. W.; Ayala, P. Y.; Morokuma, K.; Voth, G. A.; Salvador, P.; Dannenberg, J. J.; Zakrzewski, V. G.; Dapprich, S.; Daniels, A. D.; Strain, M. C.; Farkas, O.; Malick, D. K.; Rabuck, A. D.; Raghavachari, K.; Foresman, J. B.; Ortiz, J. V.; Cui, Q.; Baboul, A. G.; Clifford, S.; Cioslowski, J.; Stefanov, B. B.; Liu, G.; Liashenko, A.; Piskorz, P.; Komaromi, I.; Martin, R. L.; Fox, D. J.; Keith, T.; Al-Laham, M. A.; Peng, C. Y.; Nanayakkara, A.; Challacombe, M.; Gill, P. M. W.; Johnson, B.; Chen, W.; Wong, M. W.; Gonzalez, C.; Pople, J. A *Gaussian03*, revision D.01. Gaussian, Inc.: Wallingford, CT, 2004.

(8) Pople, J. A.; Scott, A. P.; Wong, M. W.; Radom, L. *Isr. J. Chem.* **1993**, *33*, 345.

(9) Cancès, E.; Mennucci, B.; Tomasi, J. *J. Chem. Phys.* **1997**, *107*, 3032.

(10) Mennucci, B.; Cancès, E.; Tomasi, J. *J. Phys. Chem. B* **1997**, *101*, 10506.

(11) Doering, W. von, E.; Schreiber, K. C. *J. Am. Chem. Soc.* **1955**, *77*, 514.

(12) Tuleen, D. L.; Bennett, R. H. *J. Heterocycl. Chem.* **1969**, *6*, 115.

(13) Budzelaar, P. H. M. *gNMR*, version 5.0. IvorySoft & Adept Scientific plc: Letchworth, U.K., 2004.

(14) Sasanuma, Y.; Hattori, S.; Imazu, S.; Ikeda, S.; Kaizuka, T.; Iijima, T.; Sawanobori, M.; Azam, M. A.; Law, R. V.; Steinke, J. H. G. *Macromolecules* **2004**, *37*, 9169.

(15) Sasanuma, Y. *Macromolecules* **1995**, *28*, 8629.

(16) For the method, see, for example, section 3.6 of ref. 3. In the optimization here, no weights were used.

(17) Law, R. V.; Sasanuma, Y. *Macromolecules* **1998**, *31*, 2335.

(18) Sawanobori, M.; Sasanuma, Y.; Kaito, A. *Macromolecules* **2001**, *34*, 8321.

(19) Sasanuma, Y.; Hayashi, Y.; Matoba, H.; Touma, I.; Ohta, H.; Sawanobori, M.; Kaito, A. *Macromolecules* **2002**, *35*, 8216.

(20) Brant, D. A.; Miller, W. G.; Flory, P. J. *J. Mol. Biol.* **1967**, *23*, 47.

(21) Tonelli, A. E. *J. Chem. Phys.* **1970**, *52*, 4749; *53*, 4339.

(22) Riande, E.; Guzmán, J. *Macromolecules* **1979**, *12*, 952.

(23) Inomata, K.; Phataralaoha, N.; Abe, A. *Comput. Polym. Sci.* **1991**, *1*, 126.

(24) Riande, E.; Saiz, E. *Dipole Moments and Birefringence of Polymers*; Prentice Hall: Englewood Cliffs, NJ, 1992.

(25) Nagai, K.; Ishikawa, T. *Polym. J.* **1971**, *2*, 416.

(26) Doi, M. *Polym. J.* **1970**, *3*, 252.

(27) Flory, P. J.; Fox, T. G., Jr. *J. Am. Chem. Soc.* **1951**, *73*, 1904.

(28) The word "inert" means that the polymer (or solvent) has no heteroatom to cause specific intermolecular interaction(s) distorting the chain configuration.

(29) Flory, P. J. *Pure Appl. Chem.* **1984**, *56*, 305 and references therein.

(30) See, for example: Teraoka, I. *Polymer Solutions: An Introduction to Physical Properties*; Wiley & Sons: New York, 2002.

(31) See, for example, Higgins, J. S.; Benôit, H. C. *Polymers and Neutron Scattering*; Oxford University Press: New York, 1994.

(32) Doi, M. *Introduction to Polymer Physics*; See, H., Translator; Clarendon Press: Oxford, U.K., 1996.

(33) Onsager, L. *J. Am. Chem. Soc.* **1936**, *58*, 1486.

(34) Wong, M. W.; Frisch, M. J.; Wiberg, K. B. *J. Am. Chem. Soc.* **1991**, *113*, 4776.

(35) Sasanuma, Y.; Teramae, F.; Yamashita, H.; Hamano, I.; Hattori, S. *Macromolecules* **2005**, *38*, 3519.

(36) Smits, R. G.; Koper, G. J. M.; Mandel, M. *J. Phys. Chem.* **1993**, *97*, 5745.

(37) Koper, G. J. M.; van Duijvenbode, R. C.; Stam, D. D. P. W.; Steuerle, U.; Borkovec, M. *Macromolecules* **2003**, *36*, 2500.

(38) Elias, H.-G.; Theta Solvents. In *Polymer Handbook*, 4th ed; Brandrup, J., Immergut, E. H., Grulke, E. A., Eds.; Wiley & Sons: New York, 1999; p VII/291.

(39) Flory, P. J. *Principles of Polymer Chemistry*; Cornell University Press: Ithaca, NY, 1953.

(40) Baldwin, D. T.; Mattice, W. L.; Gandour, R. D. *J. Comput. Chem.* **1984**, *5*, 241.

(41) Abe, A.; Furuya, H.; Mitra, M. K.; Hiejima, T. *Comput. Theor. Polym. Sci.* **1998**, *8*, 253.

(42) Smith, G. D.; Bedrov, D.; Borodin, O. *J. Am. Chem. Soc.* **2000**, *122*, 9548.

(43) Desiraju, G. R. Steiner, T. *The Weak Hydrogen Bond: In Structural Chemistry and Biology*; Oxford University Press: New York, 1999.

(44) Born, M.; Oppenheimer, J. R. *Ann. Phys. (Leipzig)* **1927**, *84*, 457.

(45) Sasanuma, Y.; Kumagai, R.; Nakata, K. *Macromolecules* **2006**, *39*, 6752.

MA070065N